

The Use of Satellite Constellation Geometry and A Priori Motion Constraints for Prevention of Cycle Slips in a GPS Signal Processor

Dr. Jim Sennott
Dave Senffner

Department of Electrical and Computer Engineering and Technology
Bradley University

BIOGRAPHY

Jim Sennott is Professor of Electrical and Computer Engineering at Bradley University. He received a BSEE from the U. of Delaware, and the MSEE and Ph.D. from Carnegie Mellon University. His areas of interest are optimal estimation, multiple access communications and image processing, as applied to tracking and imaging systems.

Dave Senffner is Instructor of Electrical and Computer Engineering at Bradley University. He received his BSEE and MSEE from Bradley University. His areas of interest are GPS navigation, and electronics.

ABSTRACT

For kinematic survey, and precise control of aviation, marine, and land vehicles, reliable GPS carrier phase tracking is critically important. In commercial GPS receivers, carrier phase tracking functions for individual satellites are carried out in a decoupled fashion, ignoring inter-satellite path correlations seen at the receiver antenna. Unlike traditional GPS signal processors, performance of the new coupled tracker is geometry dependent. Simulations for the complete tracking loop system illustrate how the coupled structure takes advantage of path correlations to greatly reduce phase tracking errors during periods of signal attenuation and blockage. The coupled processor is compared with the traditional processor, during simulated aircraft turning maneuvers. Cycle tracking continuity is explored for over-determined and minimal geometry scenarios. Differential correction options and computational load are also addressed.

INTRODUCTION

Carrier phase tracking is fundamental to successful GPS operations in a variety of application areas. The most critical applications involve real-time position fixing at the meter to decimeter level, which may only be obtained using the carrier phase observable, together with a differential correction scheme of some type. A variety of position fixing methods employing continuous observations of the carrier phase observable are presently in use. Among these are a) carrier smoothed pseudorange with state estimation [1,2], b) wide-lane L1/L2 ambiguity resolution [3], and c) ambiguity resolution with strongly over-determined geometry [4]. Under the assumption of high phase tracking continuity, these methods require several minutes to produce a solution at the sub-meter level. A number of techniques have been developed to cope with occasional cycle slips occurring during and after the initial "warm-up" stage.

In any navigation scheme the primary performance criteria are accuracy, availability, and integrity. In differential schemes constellation integrity is easily achieved. Attention must then turn to receiver integrity and availability. Ultimately, the challenge is to provide a satisfactory level of carrier tracking availability.

The coupled signal processor and traditional processor are first discussed. Attention is then given to relative cycle tracking and navigation performance for the two GPS receiver types. This is explored for both over-determined geometry and for minimal geometry. Finally, computational requirements and DGPS link requirements for the coupled architecture are discussed.

Traditional and Coupled GPS Processors

As shown in **Figure 1**, the traditional processor is structured around a set of parallel tracking channels, each consisting of a GPS signal correlator and reference generator. Each correlator provides raw observables to a dedicated loop filter, which in turn provides a feedback control signal to its assigned reference generator. The loop filter also provides an estimate of whole carrier phase, frequency offset, and code phase, for use in the navigation estimator. This overall architecture, of the decentralized type, is both computationally efficient and, under normal reception conditions at least, is capable of very high performance. Fundamentally, however, the tracking of signal carrier phase across the set of visible satellites in this fashion can lead to irreversible performance loss under difficult reception conditions. Fundamental performance limits for GPS signal tracking have reported in a number of studies [5,6]. In non-linear vector waveform estimation, GPS carrier phase navigation being a most important example, it is understood that jointly optimal waveform estimation can perform substantially better than well designed parallel estimators. In a recent paper [7] a preliminary attempt at developing a jointly optimal structure was reported. This coupled structure is shown in **Figure 2**.

Both the Coupled and Traditional receiver employ an identical correlator and reference generator subsystem. However, the coupled technique merges the entire in-phase and quadrature data set from the correlator bank in a jointly optimal estimator. The command vector fed back to each reference generator results from estimating the state of the correlator sub-system at the beginning of the most recent correlator interval. Also produced in the signal processor are vector estimates of signal amplitude, whole phase and frequency, and code phase. These updated estimates are transformed through geometry to obtain updated position and velocity estimates. **Appendix A** contains an overview of the estimator structure, as implemented with an extended Kalman filter whose observables are obtained directly from correlator sub-system accumulator registers.

Before describing system simulation techniques and test scenarios a few of the salient features of the coupled structure are worth noting. Fundamentally, the coupled structure fully exploits inter-satellite user-satellite statistical correlations. In the absence of these path correlations it can be shown that the traditional and coupled structures are identical in performance. In all but the most unusual of GPS carrier navigation scenarios, inter-satellite path correlations are substantial. In the navigation problems of interest path correlations are introduced by vehicle motion and clock dynamics

projected onto the collection of line-of-sight vectors. Accounting for these correlations in the phase tracking process results in a signal processor whose accuracy and cycle slippage statistics depend upon satellite geometry, as well as vehicle motion constraints, as might be encountered in 2D or guideway navigation. As will be discussed, the computational burden of the coupled signal processor is substantially greater than the traditional structure. A side benefit is the availability of the navigation solution at a very rapid update rate. Also to be addressed is the somewhat different usage of differential correction link information.

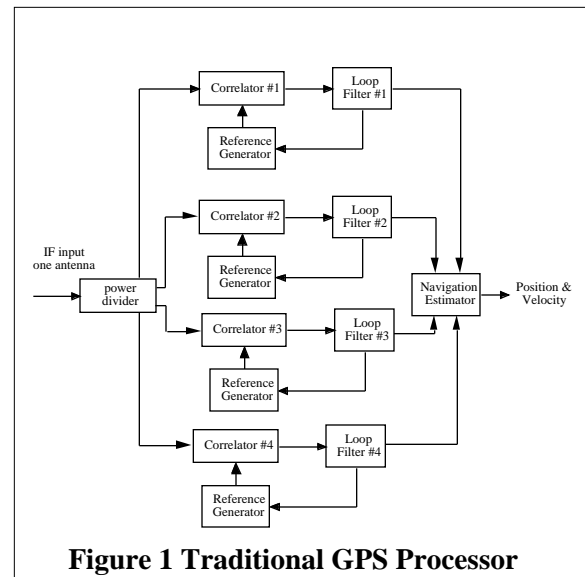


Figure 1 Traditional GPS Processor

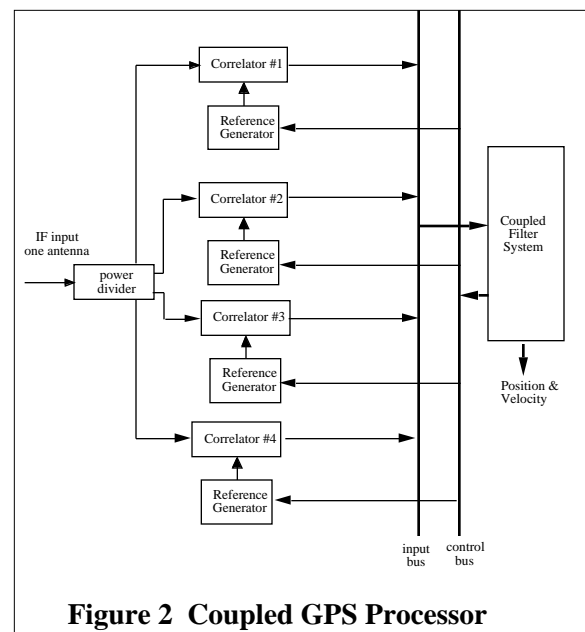


Figure 2 Coupled GPS Processor

Simulation Environment and Test Scenarios

One of the study goals was implementation of a flexible simulation interface employing a variety of resizable and movable graphical windows to assist the visualization process during and after each test run. The simulator operator can call up and place some twenty-five graphical windows across multiple monitors, describing various aspects of signal dynamics, correlator sub-system operation, tracking behavior, and vehicle navigation performance. All coding was done in "C", and implemented on the Macintosh family of computers.

Operating beneath the graphical environment is the signal simulation, whose six components are: the signal amplitude generator, the correlator sub-system, the extended Kalman filter signal amplitude, frequency and phase estimator, the navigator, and the truth trajectory generator. These elements are further discussed in **Appendix A**. A major consideration in structuring the coupled signal processor, and its simulation, is the need to model and track realistic vehicle dynamics and signal amplitude fluctuations. In the work to date, signal amplitude changes on the order of 100 dB/second have been tested. Satisfactory signal processor performance has been obtained using a signal processor and correlator update rate of 100 Hz.

An aviation-like test scenario has been extensively explored. Perhaps typical of a curved aircraft approach, or missed approach, each run begins with a constant heading segment at a ground speed of 200 knots, followed by a three degree per second turn introduced over a maneuver waypoint. At the turn onset signal attenuations commence on one or more of the visible satellites. In all cases the amplitude slew rate is 100 dB/sec. with attenuation increasing until a specified attenuation floor is reached. Signal levels then hold until the run is terminated. Runs were completed twenty seconds beyond the maneuver waypoint. To speed the computations all simulations were performed in a 2D navigation mode, with zero receiver clock. In all performance comparisons the traditional and coupled signal processors were implemented as extended Kalman filters.

Performance Comparisons, Overdetermined Geometry

A series of tests were performed with over-determined geometry. The first tests involved either three or four satellites, with an amplitude fade on a single satellite introduced at the waypoint. The satellite geometries for the two cases are shown in **Figure 3**. After initially heading in a northerly direction the aircraft began its 3 degree/second turn to the west. Simultaneously, the satellite shown in grey was rapidly attenuated. Of interest was the ability of the coupled structure to estimate and adapt its filter gains and measurement incorporations to the changing signal environment and dynamics. Several hundred runs were examined, with floor attenuations as low as -60 dB.

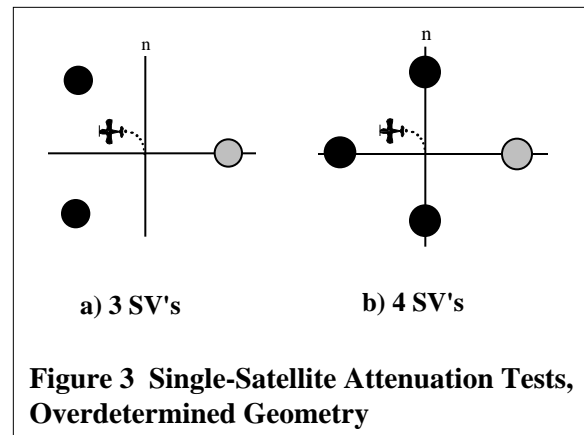
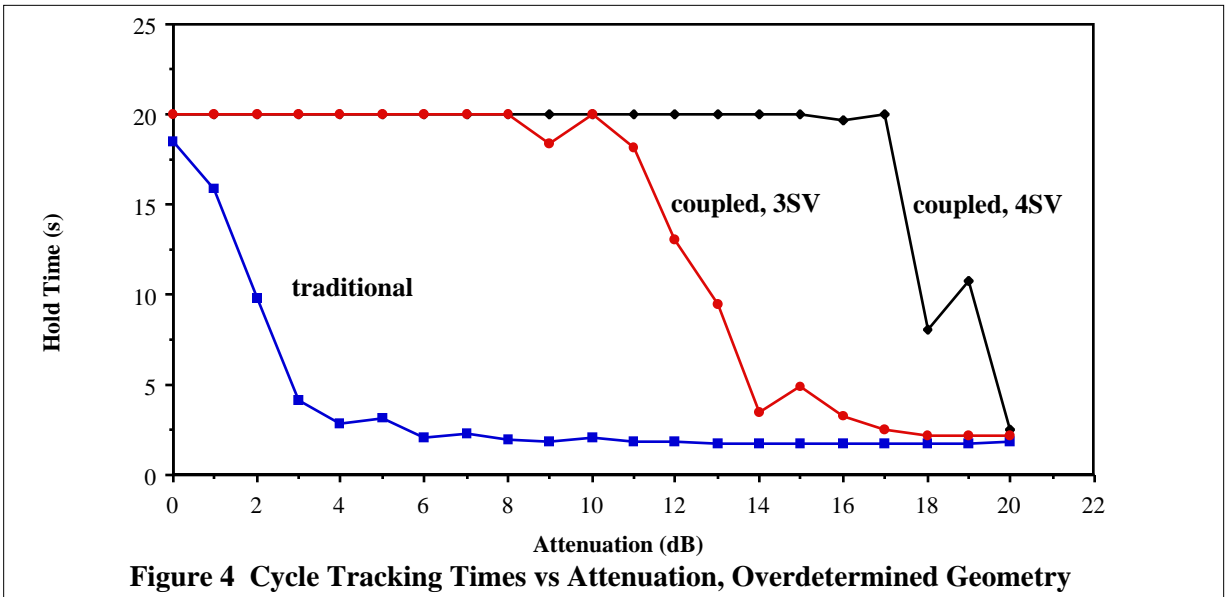


Figure 3 Single-Satellite Attenuation Tests, Overdetermined Geometry

The runs were very successful. Whereas the traditional structure soon failed to track the attenuated satellite, in both three and four satellite tests, the coupled structure maintained highly accurate phase estimates on all satellites for the entire turn.

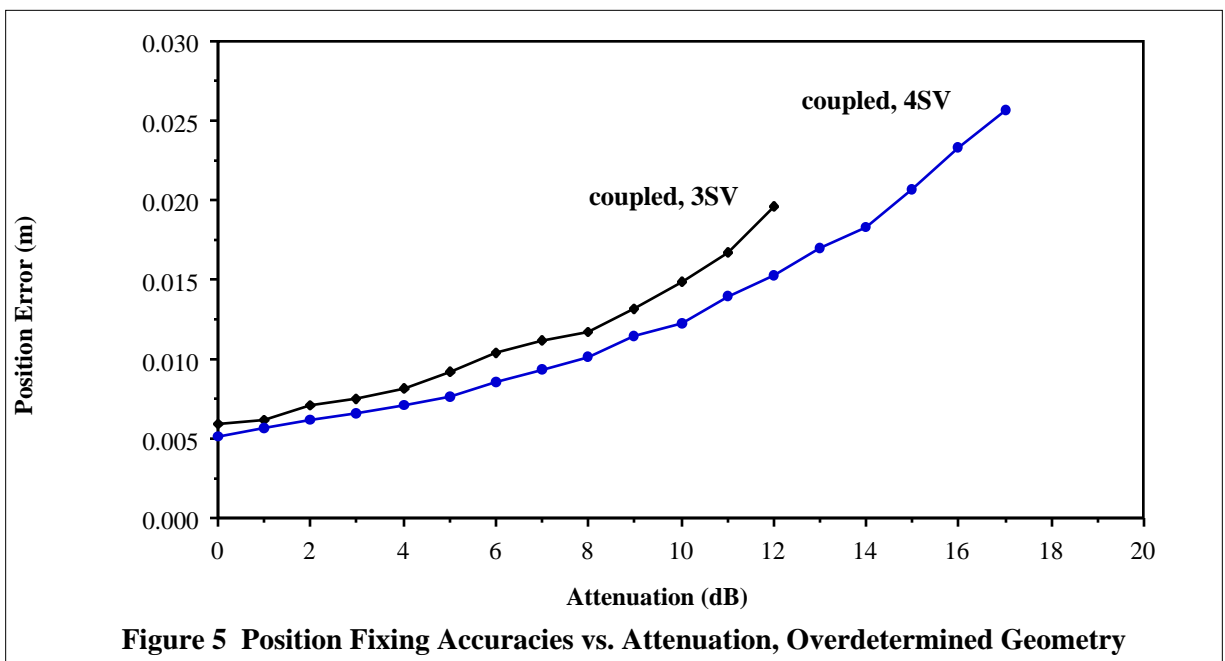
Following this series of tests, the ability to track through a constellation-wide attenuation was explored. Beginning at the turn an equal attenuation rate and attenuation floor was introduced on each satellite. The length of continuous carrier tracking following the turn/attenuation onset was of particular interest. These results are shown in **Figure 4**, with successful carrier tracking hold times plotted as a function of floor attenuation. Each data point is the result of six complete signal processor simulations observed over a turn scenario lasting twenty seconds. The improved holding times of the coupled processor are dramatically illustrated. Uncontaminated carrier tracking for the complete test interval was maintained to a level of eight to fifteen dB below that of the traditional structure, in the three and four satellite runs respectively. Not shown are the



results for two satellites, at a satellite azimuth separation of 90 degrees, for which the processors produced identical results.

The resulting errors in navigation are shown in **Figure 5**. Again, each data point represents six complete runs made at the given floor attenuation level. Only those attenuation values for which continuous carrier phase tracking was maintained during the entire twenty second turn are plotted. An underlying as-

sumption is that the carrier cycle ambiguity has been resolved prior to the turn. Furthermore, the position fixing errors do not include multipath effects, nor imperfections in the differential correction data. Generally the errors are in the low decimeter range, with a slow degradation in fix accuracy up to the point of carrier mistracking which, for the coupled structure, is reached at a floor attenuation 6 dB greater for four satellites.



Performance Comparisons, Minimum Geometry

While with over-determined geometry the coupled approach permits substantially improved continuity of signal tracking a reduced advantage is anticipated in the minimum-geometry configuration, owing to smaller inter-satellite path correlations. As will be seen, the performance benefit is strongly geometry dependent. Interestingly, for the coupled processor there is a trade-off between HDOP and carrier tracking performance, with the poorest geometry yielding the best signal tracking attenuation margin. While good geometry is generally desirable, a poorer geometry may actually produce better phase tracking during signal outage, and better navigation performance.

The geometric set-up for the two-satellite runs is shown in **Figure 6**. The unattenuated satellite was seen due east from the test location, and an attenuated satel-

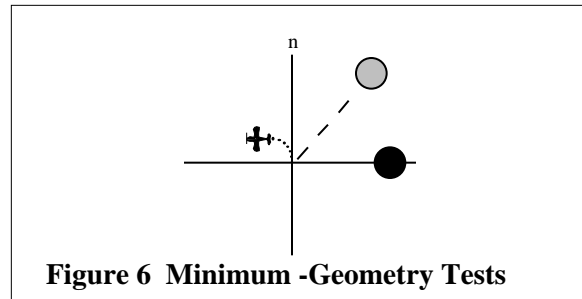


Figure 6 Minimum -Geometry Tests

While at small relative azimuths the coupled processor produces its best signal tracking performance, it must contend with large HDOP values detrimental to position fixing performance. It is therefore interesting to observe its overall position fixing performance as a function of the attenuated satellite azimuth. Results are shown in **Figure 8**, for RSS position error versus attenuation floor. As previously mentioned, it is as-

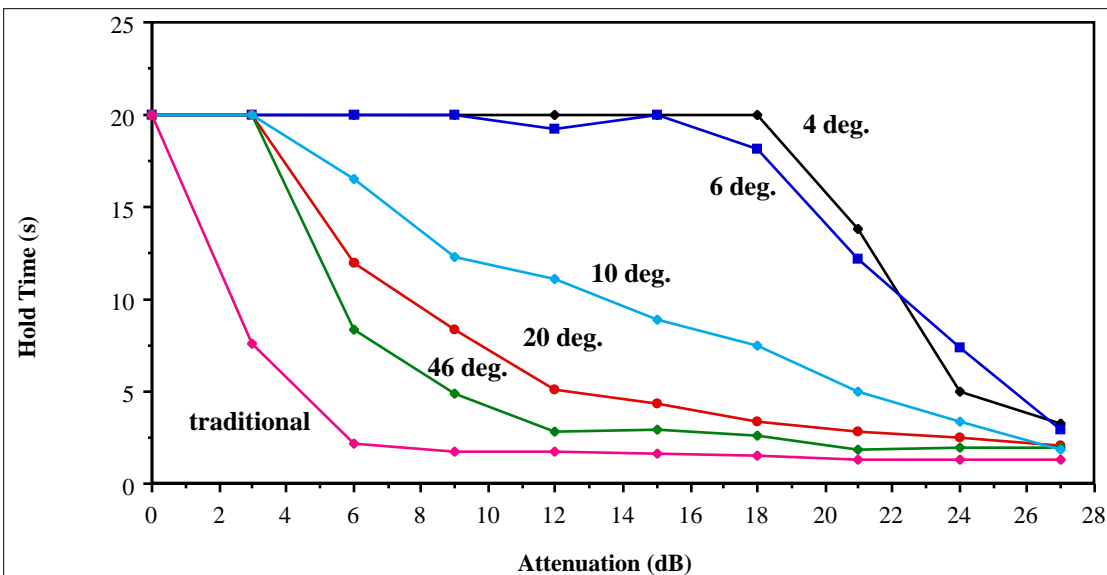


Figure 7 Cycle Tracking Times vs. Attenuation, Minimum Geometries

lite was positioned at from two to 46 degrees in a clockwise orientation from the first. As for the over-determined case signal tracking hold times from maneuver/attenuation onset were first investigated.

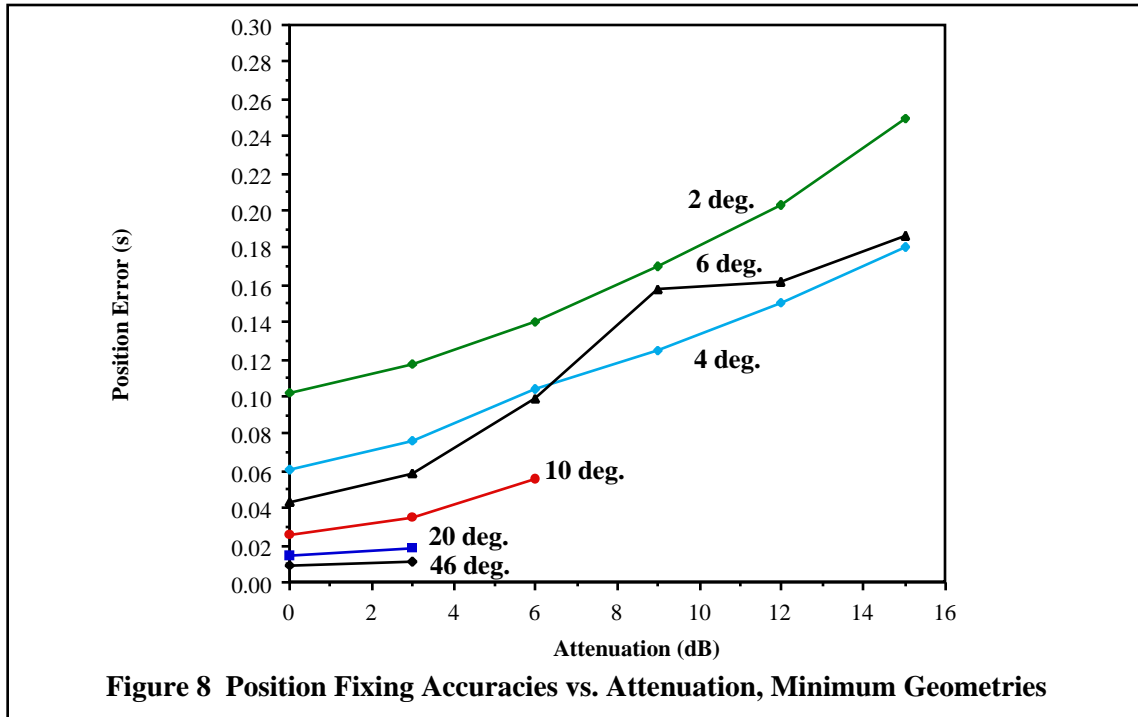
Figure 7 is a comparison of the cycle-slip free hold time for a variety of satellite azimuth angles, as a function of attenuation floor values, each data point representing the average value obtained over three to six complete runs. For azimuth values of 45 degrees or greater, the coupled system shows little advantage over the traditional structure. However, for angles below six degrees, a very large attenuation margin was observed, approaching 15 dB at the six degree azimuth. Identical results would be obtained were all azimuths increased by 180 degrees.

sumed that carrier cycle ambiguities have been resolved prior to the turn. Furthermore, the position fixing errors do not include multipath, nor imperfections in the differential correction data. These results show the interplay between geometry and signal attenuation margin. For small relative azimuths (or for relative azimuths near 180 degrees) the coupled processor offers greatly improved protection against cycle slip. Even though geometric dilution conditions are very poor navigation performance during the attenuation maneuver may be acceptable.

An interesting effect is seen in the range of four to six degrees azimuth. At small signal attenuations the better dilution of the six degree case yields better position fixing than at four degrees. However as the

attenuation floor is increased, six degree phase tracking degrades more rapidly than at four degrees, and its geometric advantage is overcome. For the traditional processor, tracking quality is independent of geometry, and its simulation and analysis is far easier.

cessing time. During field operations pre-correlator data are recorded onto a digital storage medium for later correlation and signal tracking. Data recorders based upon eight millimeter video or digital audio tape helical scan technology appear to be good candidates for this



Operational Considerations

As described previously the coupled processor is designed around the inter-path line-of-sight processes correlation model. Error sources which de-correlate these processes are detrimental to coupled processor operation. Most significant are disturbances introduced by selective availability (SA). Slowly changing effects such as ionospheric delay, and naturally occurring satellite clock and ephemeris drift are more tolerable. To counteract all these effects the coupled processor employs differential correction rates within the estimator at the time the signals are processed.

This setup is shown in **Figure 9**. In real-time operation a DGPS message of type 4 is employed. This high update rate integrated Doppler data, from a nearby reference site, is used to "rate aid" the measurement incorporation stage of the coupled processor filter.

The post-processed mode is handled quite differently from normal DGPS. Unlike conventional geodetic GPS applications, where receiver output data sets are stored for later processing, the coupled processor performs all signal correlation steps during post pro-

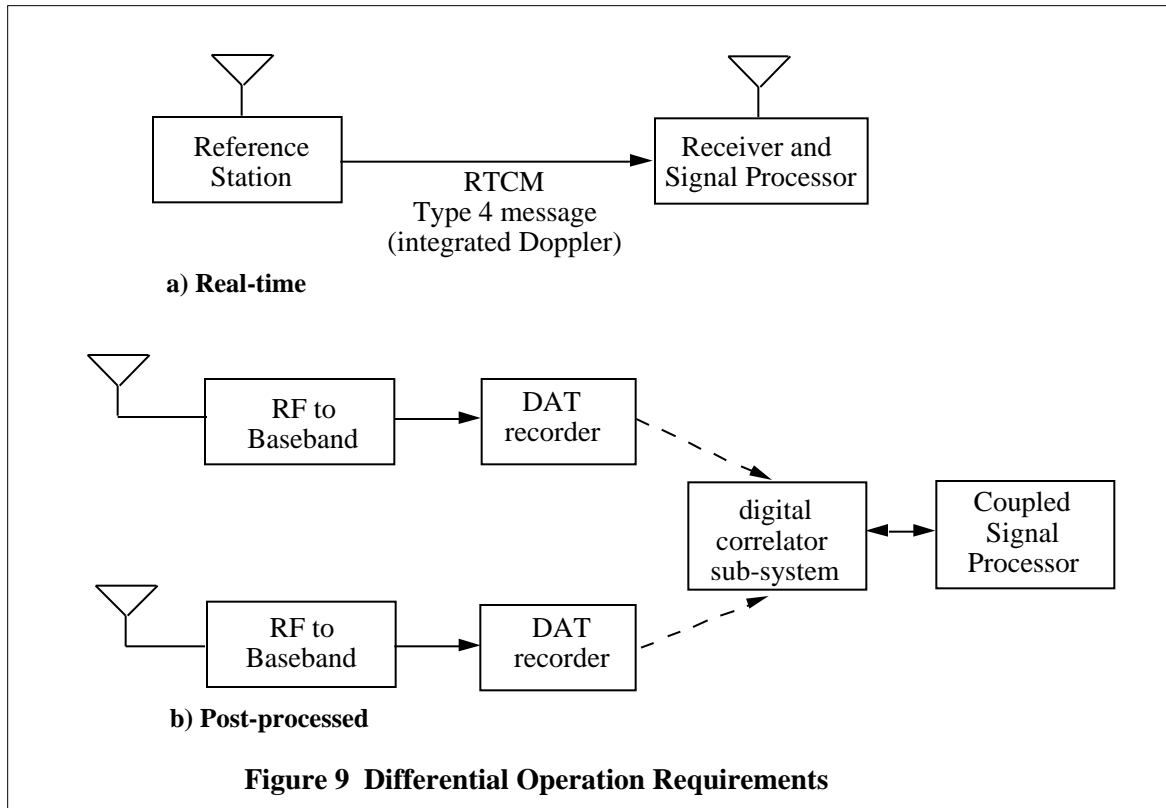
cessing requirement.

Finally the computational burden associated with the coupled processor must be addressed. To be fully effective, observation linearization, covariance propagation and gain updates are performed at the rate needed to accommodate signal amplitude fluctuations.

In contrast with the traditional GPS processor, state estimation is typically performed at rates on the order of 100 Hz, much faster than the navigation update is normally required. The computational burden is 25 to 50 times that of contemporary civilian GPS processors.

In its present implementation the coupled processor performs estimation in the line-of-sight frame of reference. Three tracker states and one amplitude state are modeled for each correlator channel. The test scenarios of this paper were run on a Motorola 68030 operating at 25 mHz. with high-speed ram cache memory. The processing rate achieved was approximately 1/20 of real-time, with the 20 second turn scenario requiring about 400 seconds to complete.

More powerful processors are currently being evaluated. A promising candidate for real-time



operation is the Motorola DSP 96002, running code optimized for vector and array operations. Benchmarks on typical array operations are impressive, with a 10-by-10 matrix floating point multiply completed in 43 microseconds. In the near future DSP processors will offer a low cost means for achieving the needed capacity.

Summary and Conclusions

Unlike the traditional GPS structure, performance is geometry dependent, with additional satellites impacting the signal tracking performance of the overall receiver. The coupled processor architecture offers substantial improvement in carrier tracking availability and accuracy in difficult signal reception environments, with and without overdetermined satellite geometry. Further performance enhancement is available when vehicle motion is constrained, as for example in 2D marine or vehicle guideway operations.

To counteract the decorrelation of inter-satellite path dynamics due particularly to the selective availability error source, the coupled structure employs differential rate corrections derived from reference sta-

tion carrier data within its signal tracking stages.

Finally, the coupled processor requires no modification to the correlator sub-system of present-day GPS receivers, and in the near future the needed computational throughput can be obtained at reasonable cost with DSP processors.

References

- [1] Hwang, Y.C., Kinematic GPS: Resolving Integer Ambiguity on the Fly, Proceedings IEEE Position Location and Navigation Symposium, March 1990, pp. 579-586.
- [2] Sennott, J.W., and Spalding, J., Multipath Sensitivity and Carrier Slip Tolerance of an Integrated Doppler DGPS Navigation Algorithm, Proceedings IEEE Position Location and Navigation Symposium, March 1990, pp. 638-644.
- [3] Hatch, R., Ambiguity Resolution in the Fast Lane, Proceedings of ION GPS-89, Colorado Springs, September 1989, pp. 45-50.
- [4] Goad, C., Optimal Filtering of Pseudoranges and Phases from Single Frequency GPS Receivers,

Navigation, Vol. 37, Fall 1990, pp. 249-262.

[5] Sennott, J., Dynamical Errors For GPS C/A Demodulation/Navigation Processors Subject to Signal Failure and Maneuver-Induced Attenuation, DOT Report TSC-RS117-PM-81-19, September 1981.

[6] Sennott, J., Fault/Maneuver Tolerance of Aided GPS Demodulation Navigation Processors in Precision Aviation Applications, Proceedings of Institute of Navigation National Aerospace Meeting, March 1982.

[7] Senffner, D., A Coupled-Channel Phase Tracking System for Improved GPS Carrier Navigation During Signal Outage, Presented at ION GPS-90, September 1990.

Appendix A Signal Processor Development

Navigation State Model

In keeping with the desire for simplicity, only two-dimensional motion is considered and user clock dynamics are suppressed. This model was used to formulate the dynamics of the line-of-sight from each satellite to the user and to describe the phase and frequency inputs to each of the correlators. The general form of the discrete time navigation model is shown below:

$$\underline{X}_{k+1} = p \underline{X}_k + \underline{W}_{k,p} \quad (\text{A-1})$$

where:

$$\underline{X}_p = \begin{bmatrix} X_{1p} \\ X_{2p} \\ X_{3p} \\ X_{4p} \end{bmatrix}$$

and in the subsequent development the user position components will be denoted as:

Navigation Signal Development

A typical two-dimensional motion model and satellite geometry is shown in **Figure A-1**. where:

- P = position of the user
- S_i = position of satellite number i
- V_{iu} = component of the user's velocity in the direction of satellite number i

The signal development is for satellite #1. As stated previously, no telemetry data or signal envelope is assumed on the carrier. The received signal for correlator one is:

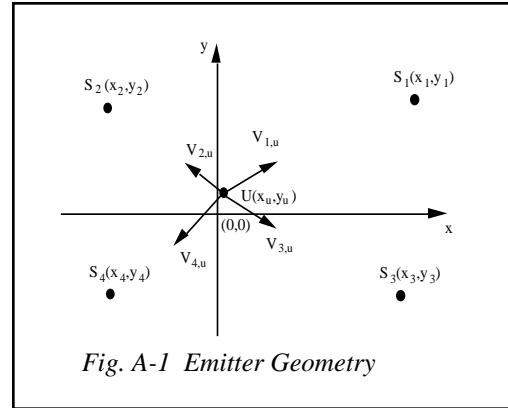


Fig. A-1 Emitter Geometry

where:

$$R_{c1}(t) = A_1(t) \cos [c_1(t - \tau_1(t))]$$

A₁(t) = amplitude of the carrier signal for channel 1

c₁ = carrier frequency

τ₁(t) = propagation delay as seen by channel 1

with

and C = speed of light. The displacements can be

$$\tau_1(t) = \frac{\sqrt{(x_1 - x_u)^2 + (y_1 - y_u)^2}}{C}$$

expressed in vector form as:

A Taylor's Series Expansion is used to represent the

$$R_{c1}(t) = A_1(t) \cos c_1 t - \frac{|\underline{x}_1 - \underline{x}_u|}{c}$$

delay term over the signal correlation interval:

The following terms are used to simplify the above;

$$|\underline{x}_1 - \underline{x}_u| = |\underline{x}_1 - \underline{x}_u(t)|$$

$$|\underline{x}_1 - \underline{x}_u(t_0)| + \frac{d}{dt} \{ |\underline{x}_1 - \underline{x}_u(t_0)| \} (t - t_0)$$

The reference signal is defined as R_{ref} = cos c₁t and the

$$c_1 \left(1 - \frac{V_{1,u}}{c} \right) - \frac{c_1}{c} |\underline{x}_1 - \underline{x}_u(t_0)| + \frac{c_1}{c} V_{1,u} t_0$$

$$V_{1,u} = \frac{d}{dt} \{ |\underline{x}_1 - \underline{x}_u(t_0)| \}$$

the “whole” phase and frequency values are defined relative to the reference as:

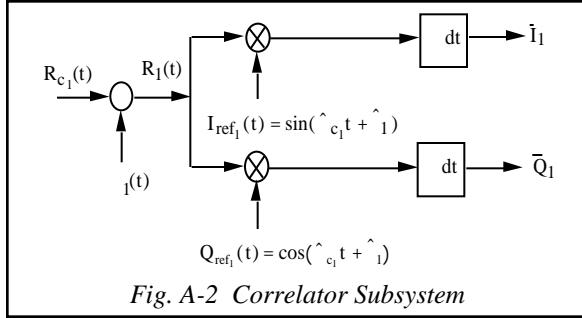
Four line-of-sight paths are defined and hence,

$$1 \quad c_1 - c_1 = c_1 \frac{V_{1,u}}{c}$$

$$1 \quad 0 - = \frac{c_1}{c} [\bar{x}_1 - \bar{x}_u(t_o)] - \frac{c_1}{c} V_{1,u} t_o$$

four correlators. The correlator model development follows. The notation employed in the development is for channel 1. A block diagram of the channel 1 correlator is shown below. This correlator implementation is of the analog type. An equivalent digital version consists of shared sine and cosine references, balanced mixers, low-pass filters and A/D converters, followed by sine and cosine multiply and accumulate elements.

$i(t)$ is additive white Gaussian with power



spectral density watts/Hz. Closed form expressions for the mean and variance for I and Q outputs are readily derived and are given below:

Correlator State Variables

$$E[I_1] = \frac{A_1}{2(c_1 - \hat{c}_1)} \left\{ \cos[(c_1 - \hat{c}_1)(k+1)T_c + (c_1 - \hat{c}_1)] - \cos[(c_1 - \hat{c}_1)kT_c + (c_1 - \hat{c}_1)] \right\}$$

$$E[Q_1] = \frac{A_1}{2(c_1 - \hat{c}_1)} \left\{ \sin[(c_1 - \hat{c}_1)(k+1)T_c + (c_1 - \hat{c}_1)] - \sin[(c_1 - \hat{c}_1)kT_c + (c_1 - \hat{c}_1)] \right\}$$

$$\frac{2}{I_1} = \frac{1T_c}{4}$$

$$\frac{2}{Q_1} = \frac{1T_c}{4}$$

The correlator state at the kth. time step will be defined as the offset in phase and frequency at the start of the kth. correlation interval. During the correlation interval this state is perturbed by the line-of-sight motion noise and by any correlator control input. The correlator state model is written as:

$$\underline{X}_{cor}(k) = \underline{A}_{cor} \underline{X}_{cor}(k-1) + \underline{W}_{k,los} + \underline{U}_{cor}(k)$$

where:

$$\underline{X}_{cor}(k) = \begin{bmatrix} X_{corr1} \\ X_{corr2} \\ X_{corr3} \\ X_{corr4} \end{bmatrix}$$

$$\underline{X}_{corr_i} = \begin{bmatrix} e_i(k) \\ e_i(k) \end{bmatrix}$$

with each submatrix given as:

and $\underline{U}_{cor}(k) = -\hat{\underline{X}}_{cor}(k-1)$ with the correlator control given by:

$$\underline{cor} = \begin{bmatrix} 1 & 0 & 0 & 0 \\ 0 & 2 & 0 & 0 \\ 0 & 0 & 3 & 0 \\ 0 & 0 & 0 & 4 \end{bmatrix}$$

The correlator state transition matrix is given by:

with each submatrix being:

$$i = \begin{bmatrix} 1 & T_c \\ 0 & 1 \end{bmatrix}$$

Next the covariance of $\underline{W}_{k,los}$ is developed. Consider the transformation between the navigation and the line-of-sight frames:

$$\underline{X}_{LOS}(k) = \underline{h}_g[\underline{X}_p(k)]$$

where:

$\underline{X}_{LOS}(k)$ = 1x8 phase/frequency vector
 \underline{h}_g = non-linear vector function
 $\underline{X}_p(k)$ = 1x4 user state vector consisting of position and velocity

Relative to some nominal position, the line-of-sight vector is defined as:

$$\underline{X}_{LOS}(k) = \underline{h} \left[\underline{X}_{p,nom}(k) + \underline{X}_p(k) \right]$$

$$= \underline{X}_{LOS,nom}(k) + \underline{X}_{LOS}(k)$$

$$\underline{X}_{LOS,nom}(k) + \underline{H}_g \underline{X}_p(k) \left\{ \underline{X}_p(k) \right\}$$

where

$$\underline{X}_{LOS,nom} = \underline{h} \left| \underline{X}_{p,nom}(k) \right.$$

$$\underline{X}_{LOS}(k) = \underline{H}_g \underline{X}_p(k)$$

$$\underline{H}_g = \underline{X}_p \underline{h} \left| \underline{X}_{p(t_0)} \right.$$

$$\underline{H}_g = \begin{bmatrix} h_1 \\ h_2 \\ h_3 \\ h_4 \end{bmatrix}$$

$$h_i = \begin{bmatrix} \frac{i}{x} & 0 & \frac{i}{y} & 0 \\ 0 & \frac{i}{\dot{x}} & 0 & \frac{i}{\dot{y}} \end{bmatrix}$$

$$h_i = \begin{bmatrix} -\frac{c}{c} \frac{(x_i - x_u)}{i} & 0 & -\frac{c}{c} \frac{(y_i - y_u)}{i} & 0 \\ 0 & \frac{c}{c} \frac{(x_i - x_u)}{i} & 0 & \frac{c}{c} \frac{(y_i - y_u)}{i} \end{bmatrix}$$

$$Q_p = \begin{bmatrix} p & 0 \\ 0 & p \end{bmatrix}^T (T -) Q_s \begin{bmatrix} p & 0 \\ 0 & p \end{bmatrix}^T (T -) d$$

The pertinent positions in the H matrix are formed as shown below:

with each h_i given as:

The derivatives with respect to position and velocity are:

The discrete-time covariance matrix for the navigation model was determined from:

where Q_s is the power spectral density matrix associated

$$\underline{W}_{k,los} = \underline{H}_g \underline{W}_{k,p}$$

with the vehicle dynamics. Arrays Q_s and p were

$$Q_k = \underline{H}_g Q_p \underline{H}_g^T$$

adjusted to model the desired navigation velocity process. This in turn controls the changes as seen by the correlator system across a time step. The process noise as seen

$$\underline{Z}(k) = \underline{h}_c \left| \underline{X}(k) \right. + \underline{V}(k)$$

along the line-of-sight path is defined as:

$$\underline{h}_c \left| \underline{X}(k) \right. = \begin{bmatrix} E[I_1] \\ E[Q_1] \\ M \\ M \\ E[I_4] \\ E[Q_4] \end{bmatrix}$$

This then gives for the correlator state model proces

$$\underline{V}(k) = \begin{bmatrix} V_1(k) \\ V_2(k) \\ M \\ M \\ V_8(k) \end{bmatrix}$$

noise covariance:

Note that Q_k is in general not going to be block diagonal.

$$R_k = \begin{bmatrix} w^2 & 0 & L & L & 0 \\ 0 & w^2 & & & M \\ M & & O & & M \\ M & & & O & M \\ 0 & L & L & L & w^2 \end{bmatrix}$$

Observation Equations

$$\underline{H}_{cor}(k) = \underline{X}_{cor} \underline{h}_c \left| \underline{X}_{-cor}(k) \right.$$

$$= \begin{bmatrix} H_1 & 0 & L & 0 \\ 0 & H_2 & & M \\ M & & H_3 & M \\ 0 & L & L & H_4 \end{bmatrix}$$

The observation equation is given by:

$$H_i = \begin{bmatrix} \frac{\dot{I}_i}{\bar{Q}_i} & \frac{\dot{I}_i}{\bar{Q}_i} \\ \frac{e_i}{e_i} & \frac{e_i}{e_i} \end{bmatrix}$$

where
with

The observation noise vector $\underline{V}(k)$ is statistically white, and has the variance values previously developed.

In developing the extended Kalman filter the linearization matrix H_c is computed as:

with each H_i a 2x2 submatrix as given below:

Signal Processor Operations

Fig. A-3 describes the components of the Coupled Filter. This device is fed by the correlator input and control bus data lines. Additionally, in the case of a remote site correction station, correction data may also be applied. There are seven components in the coupled filter. The simplest of these are conventional PSK telemetry bit detectors and signal amplitude

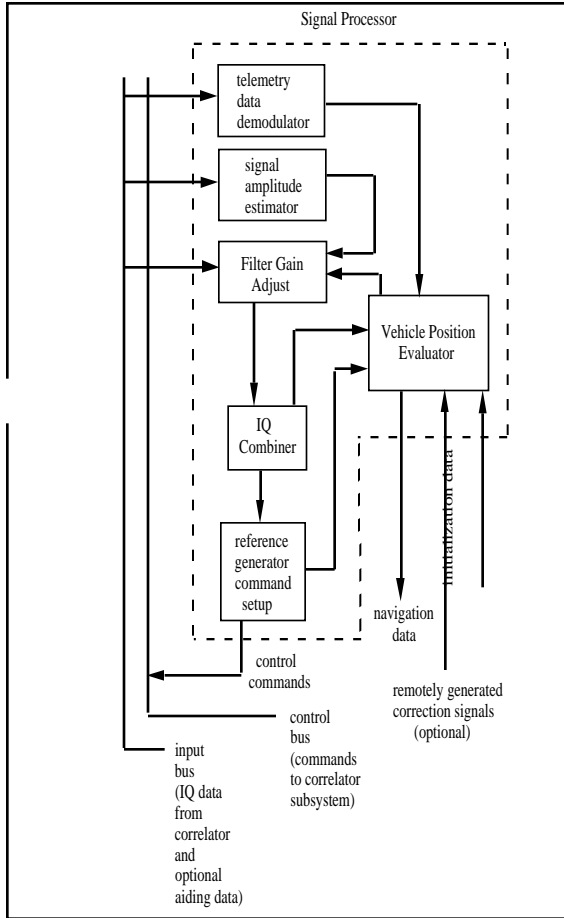


Fig. A-3 Coupled Signal Processor Components

estimators, each fed by the raw correlator IQ data stream from the correlator sub-system. These are responsible for recovery of GPS telemetry data impressed upon each of the transmitted L-band carriers, and for maintaining current estimates of fluctuating signal amplitudes, respectively.

Signal Amplitude Estimator Development

This component reads the raw correlator data vector and produces estimates of signal amplitude. There are two processing steps that are performed here. In order for the signal process to properly adapt to changing signal quality conditions observed at the vehicle antenna(s) it is necessary that signal amplitude estimates be updated at a rapid rate, typically every 10 milliseconds. These estimates are later used by the Filter Gain Adjust. The first step is to read the most recent correlator data values, as provided from the input data bus. Referring to the observation equation, the input data elements to be processed are “I” and “Q”. In the second step an updated amplitude estimate for each satellite line-of-sight path is then computed. To this end the “I” and “Q” values for the on-time code reference correlator are

scaled and sum-squared. These estimates are then fed into an IIR filter for smoothing.

The most important elements of the processor are contained in the sub-components labeled Filter Gain Adjust and IQ Combiner. The Filter Gain Adjust is responsible for maintaining a dynamic set of weighting coefficients used in the subsequent IQ Combining component, where the latest set of correlator data are merged to form correlator reference waveform positioning error estimates referenced to the previous correlation interval.

Filter Gain Adjust Component

Fundamental to the Filter Gain Adjust component is the generation of a covariance matrix which describes in a statistical fashion the relationship between motions across the complete set of EF-BF line-of-sight paths. This is kept up-to-date using approximate geometric information maintained by the Vehicle Position Evaluator. Geometric information is developed in a conventional manner within the Vehicle Position component. From these estimates an approximate set of direction cosine estimates for all EF-BF paths of interest is next generated. This data, together with a pre-set nominal statistical model for vehicle translation rate is then fed to the Filter Gain Adjust component. Within this component the covariance matrix of line-of-sight perturbations is computed, followed by update of a filter gain array, subsequently used in the IQ Combiner. The Filter Gain Adjust component used for this paper is an Extended Kalman Filter. It provides an estimate of correlator states, i.e. phase error and frequency errors, which are in turn used to provide whole phase and whole frequency offset terms. The measurements are the in-phase and quadrature terms “I” and “Q” as derived previously. These are highly non-linear; hence the need for the Extended Kalman Filter as opposed to a Linear Kalman Filter. Linearization of these observables to first-order is performed at every new measurement.

$$\hat{\underline{X}}_{\text{cor}}^-(k) = \text{cor} \hat{\underline{X}}_{\text{cor}}^+(k-1) - \underline{U}(k-1)$$

While higher-order linearization schemes have been

$$\underline{P}^-(k) = \text{cor} \underline{P}^+(k-1) \underline{T}_{\text{cor}}^T + \underline{Q}_k(k-1)$$

proposed for non-linear estimation, the first-order expansion appears to capture the essence of multi-emitter phase tracking in navigation. The first step is to perform state extrapolation with the most recent correlator update as:

Then the error covariance matrix was extrapolated as:
The residuals are then computed by subtracting the

$$K(k) \approx P^-(k) H_{cor}(k)^T [H_{cor}(k) P^-(k) H_{cor}(k)^T + R(k)]^{-1}$$

current I and Q data from the predicted I and Q data. Next the correlator sub-system, which is highly non-linear in the operating region of interest, is linearized

$$P^+(k) = [I - K(k) H_{cor}(k)] P^-(k)$$

about the current estimate of the correlator state vector as shown below previously. Then the filter gain is computed as:

After the filter gain is computed, the error covariance matrix is updated using the standard Kalman filter methodology.

IQ Combiner

$$\hat{\underline{X}}_{cor}^+(k) = \hat{\underline{X}}_{cor}^+(k) + K(k) [\underline{Z}(k) - \hat{\underline{Z}}(k)]$$

The IQ Combiner extrapolates its most recent correlator reference waveform positioning error estimates to the time tag of the new batch of IQ data supplied across the correlator input bus. It then incorporates a new state vector for the correlator by using the filter gain derived and the residuals.

The waveform positioning error estimates are then updated and fed to the correlator reference generator command setup component.

Vehicle Position Evaluator

In the Vehicle Position Evaluator extrapolated line-of-sight values and linearized geometry are used to generate the least-squared-error estimate of navigation states. This data may be sent to an external display or

$$\hat{\underline{X}}_{los}(k+1) = \hat{\underline{X}}_{los}(k) - \underline{X}_{los,nominal}$$

$$\hat{\underline{X}}_p = \hat{\underline{X}}_{p,nominal} H_g^{-1} \hat{\underline{X}}_{los}$$

storage device, depending upon the application. For this paper the data was stored and later used to determine position error. Applying the geometry linearization previously developed, the following equations are used to transform from the line-of-sight estimates of phase and frequency back to position and velocity.

In the examples of this paper H is 8x4 and the mapping

$$H^\# = (H^T H)^{-1} H^T$$

from the line-of-sight domain into the position domain is over-specified. Since a least-square estimate is desired the pseudo-inverse of H is employed. The pseudo-inverse of H is defined as:

Reference Generator Setup

The reference setup provides control signal which are fed back to the correlators. Because of setup resolution limitations in typical correlator subsystems to which the signal processor may be interfaced, provisions are made within the signal processor for error setpoints which are non-zero. In a conventional GPS correlator subsystem, the code generator will only be programmable in fractional code chip steps. Likewise the numerically controlled oscillator (NCO) in a typical GPS correlator will be settable to a value much coarser than the precision of the values maintained in the signal processor. To account for these effects, provisions are made in the signal processor for non-zero set-points.

In a more practical signal processor the satellite positions and velocities would be introduced. Also, if an externally supplied differential correction from a DGPS reference station was available it would be applied in this step.